1 **Adenosine receptor and its downstream targets, mod(mdg4) and Hsp70, work as a**
2 **signaling pathway modulating cytotoxic damage in *Drosophila***

3 Yu-Hsien Lin[1,2,*,¥], Houda Ouns Maaroufi[1,2], Lucie Kucerova[1], Lenka Rouhova[1,2], Tomas
4 Filip[1,2], Michal Zurovec[1,2*]

5 [1]Biology Centre of the Czech Academy of Sciences, Institute of Entomology, Ceske
6 Budejovice, Czech Republic, [2]Faculty of Science, University of South Bohemia, Ceske
7 Budejovice, Czech Republic,

8

9 *Correspondence and requests for materials should be addressed to Y.H.L. (email:
10 r99632012@gmail.com) and M.Z. (email: zurovec@entu.cas.cz).

11 ¥Current address: Department of Plant Physiology, Swammerdam Institute for Life
12 Sciences, University of Amsterdam, 1098 XH Amsterdam, The Netherlands

13 **Summary**

14 Adenosine (Ado) is an important signaling molecule involved in stress responses. Studies
15 in mammalian models have shown that Ado regulates signaling mechanisms involved in
16 'danger-sensing' and tissue-protection. Yet, little is known about the role of Ado
17 signaling in *Drosophila*. In the present study, we observed lower extracellular Ado
18 concentration and suppressed expression of Ado transporters in flies expressing mutant
19 huntingtin protein (mHTT). We altered Ado signaling using genetic tools and found that
20 the overexpression of Ado metabolic enzymes, as well as the suppression of Ado receptor
21 (AdoR) and transporters (ENTs), were able to minimize mHTT-induced mortality. We
22 also identified the downstream targets of the AdoR pathway, the modifier of mdg4
23 (Mod(mdg4)) and heat-shock protein 70 (Hsp70), which carry out its function. Finally,
24 we showed that a decrease in Ado signaling affect other *Drosophila* stress reactions,
25 including paraquat and heat-shock treatments. Our study provides important insights into
26 how Ado regulates stress responses in *Drosophila*.

Introduction

28   Tissue injury, ischemia, and inflammation activate organismal responses involved
29 in the maintenance of tissue homeostasis. Such responses require precise coordination
30 among the involved signaling pathways. Adenosine (Ado) represents one of the key
31 signals contributing to the orchestration of cytoprotection, immune reactions, and
32 regeneration, as well as balancing energy metabolism (Borea et al., 2016). Under normal
33 conditions, the Ado concentration in blood is in the nanomolar range; however, under
34 pathological circumstances the extracellular Ado (e-Ado) level may dramatically change
35 (Moser et al., 1989). Ado has previously been considered a retaliatory metabolite, having
36 general tissue protective effects. Prolonged adenosine signaling, however, can exacerbate
37 tissue dysfunction in chronic diseases (Antonioli et al., 2019) Ado therefore functions as
38 an imperfect protector; in some cases it may be beneficial, while in others it may worsen
39 tissue damage (Picano and Abbracchio, 2000).

40   Ado signaling is well-conserved among phyla. The concentration of Ado in the *D.*
41 *melanogaster* hemolymph is maintained in the nanomolar range, as in mammals, and
42 increases dramatically in adenosine deaminase mutants or during infections (Dolezelova
43 et al., 2005;Novakova and Dolezal, 2011). Unlike mammals, *D. melanogaster* contains
44 only a single AdoR isoform (stimulating cAMP) and several proteins that have Ado
45 metabolic and transport activities involved in the fine regulation of adenosine levels.
46 *Drosphila melanogaster* adenosine deaminase-related growth factors (ADGFs), which
47 are related to human ADA2, together with adenosine kinase (AdenoK) are the major
48 metabolic enzymes converting extra- and intra-cellular adenosine to inosine and AMP,
49 respectively (Zurovec et al., 2002;Maier et al., 2005;Stenesen et al., 2013). The transport
50 of Ado across the plasma membrane is mediated by three equilibrative and two
51 concentrative nucleoside transporters (ENTs and CNTs, respectively) similar to their
52 mammalian counterparts. Ado signaling in *Drosophila* has been reported to affect various
53 physiological processes, including the regulation of synaptic plasticity in the brain,
54 proliferation of gut stem cells, hemocyte differentiation, and metabolic adjustments
55 during the immune response (Knight et al., 2010;Mondal et al., 2011;Bajgar et al.,
56 2015;Xu et al., 2020).

57   The present study examined the role of *Drosophila* Ado signaling on cytotoxic

58   stress and aimed to elicit the underlying mechanism. Earlier reports have shown that

59   expression of the expanded polyglutamine domain from human mutant huntingtin protein

60   (mHTT) induces cell death in both *Drosophila* neurons and hemocytes (Marsh et al.,

61   2000;Lin et al., 2019). In our study, we confirmed the low-viability phenotype of mHTT-

62   expressing larvae and observed that such larvae display a lower level of e-Ado in the

63   hemolymph. Furthermore, we used genetic tools and altered the expression of genes

64   involved in Ado metabolism and transport to find out whether changes in Ado signaling

65   can modify the phenotype of mHTT-expressing flies. Finally, we uncovered a

66   downstream mechanism of the *Drosophila* Ado pathway, namely *mod(mdg4)* and Hsp70,

67   which modify both the formation of mHTT aggregates and the stress response to heat-

68   shock and paraquat treatments.

69

Results

Decreased hemolymph Ado titer in mHTT-expressing larvae

72   To characterize the involvement of Ado signaling in the stress response, we used mHTT-

73   expressing flies as a well-characterized genetic model for neurodegeneration and

74   cytotoxic stress (Rosas-Arellano et al., 2018). We initially examined flies overexpressing

75   normal exon 1 from human huntingtin (Q20 HTT), or its mutant pathogenic form (Q93

76   mHTT), driven by the ubiquitous *daughterless-Gal4* (*da-Gal4*) and pan-neuron driver

77   (*elav-Gal4*). We observed that 100% of Q93-expressing larvae driven by *da-Gal4* died

78   during the wandering stage. In contrast, those driven by *elav-Gal4* displayed no impact

79   on larval development (Fig. S1A) but with a reduced adult eclosion rate (Fig. S1B) and

80   lifespan (Fig. S1C). These results are consistent with previous observations (Song et al.,

81   2013).

82   Measurement of the extracellular Ado (e-Ado) concentration in the hemolymph of Q93-

83   expressing larvae (3rd instar) showed that its level was significantly lower compared to

84   larvae expressing Q20 or control *da-GAL4* only (Fig. 1A). Since e-Ado concentration

85   may be associated with the level of extracellular ATP (e-ATP), we also examined its titer

86   in larval hemolymph. However, as shown in Fig. 1B, there was no significant difference

87   in e-ATP levels between Q20, Q93, and control *da-GAL4* larvae.

88   We thus postulated that the lower level of e-Ado in Q93 larvae might be caused by

89   changes in genes involved in Ado metabolism or transportation. Therefore, we compared

90   the expression of *adgf* genes (*adgf-a*, *adgf-c*, *adgf-d*), adenosine kinase (*adenoK*),

91   adenosine transporters (*ent1*, *ent2*, *ent3*, *cnt2*), and adenosine receptor (*adoR*) in the

92   brains of Q93- and Q20-expressing larvae driven by *elav-Gal4* (Fig. 1C). The results

93   showed that the expression levels of *adgf-a* and *adgf-d*, as well as transporters *ent1*, *ent2*,

94   and *ent3*, in the brain of Q93 larvae were significantly lower than in Q20 larvae. There

95   was no difference in the expression of *cnt2* and *adoR* between Q93 and Q20 larvae.

96   **Enhanced e-Ado signaling increased mortality of mHTT flies**

97   To study the effect of e-Ado signaling on mHTT-induced cytotoxicity, we compared the

98   survival of transgenic lines that co-express RNAi constructs of Ado metabolic, transport

99   and receptor genes together with Q93 and Q20 driven by *elav-GAL4*. The results showed

100   that knocking down *adgf-D*, *ent1*, *ent2*, and *adoR* resulted in a significantly increased

101   eclosion rate (Fig. 1D), and silencing *adgf-A* and *adenoK*, *ent1*, *ent2*, and *adoR*

102   significantly extended the adult lifespan of mHTT-expressing flies (Fig. 1E). Notably, the

103   RNAi silencing of *ent2* and *adoR* extended the lifespan of mHTT-expressing flies to 30

104   and 40 days, respectively, which is about 1.5~2 times longer than that of control *gfp-*

105   RNAi-expressing mHTT flies. To ensure that the mortality of the Q93 flies was mainly

106   caused by mHTT expression and not by the RNAi constructs, we examined the survival

107   of flies co-expressing normal htt Q20 together with RNAi transgenes until all

108   corresponding experimental flies (expressing Q93 together with RNAi constructs) died.

109   We did not observe a significant effect for any of the RNAi transgenes on adult survival

110   (Fig. S2).

111   It is generally assumed that gain- and loss-of-function manipulations of functionally

112   important genes should lead to the opposite phenotypes. We therefore tested whether

113   the overexpression of *adgf-A*, *adenoK*, *ent2*, and *adoR* would rescue mHTT phenotypes.

114   As shown in Fig. 1F, increasing either the intra- or extracellular Ado metabolism by

115   overexpressing *adenoK* and *adgf-A* in Q93 flies extended their lifespan in comparison to

4

116 control Q93 flies overexpressing GFP protein. In contrast, the overexpression of *ent2* and

117 *adoR* significantly decreased the lifespan of mHTT-expressing flies. Therefore, the

118 overexpression of *adoR* and *ent2* genes resulted in a phenotype opposite to that observed

119 in the knockdowns, thus supporting the importance of these genes as key regulators of

120 mHTT phenotypes.

121 **Knocking down *ent2* and *adoR* reduced cell death and mHTT aggregate formation**

122 To determine whether the reduction of Ado signaling could affect other phenotypes of

123 Q93 flies, we examined the effect of knocking down genes involved in Ado signaling and

124 metabolism on *Drosophila* rhabdomere degeneration and mHTT aggregate formation.

125 We expressed RNAi transgenes in the eyes of Q93 flies using the *gmr-GAL4* driver

126 (Mugat et al., 2008;Kuo et al., 2013) and compared the levels of retinal pigment cell

127 degeneration (Fig. 2A). The results revealed that silencing Ado metabolic enzymes did

128 not significantly influence the level of retinal pigment cell degeneration; however, retinal

129 pigment cell degeneration was significantly reduced in *ent2* knockdown flies.

130 Surprisingly we did not observe a significant rescue of cell death by silencing *adoR* (Fig

131 S3). We therefore assumed that it might be due to insufficient RNAi efficiency for

132 suppressing AdoR signaling in the eye. To test this, we examined two combinations:

133 mHTT-expressing flies with the adoR RNAi transgene under an adoR heterozygous

134 mutant background (AdoR^1/+), and mHTT-expressing flies under an AdoR^1 homozygous

135 mutant background. As shown in Fig. 2A, both had significantly rescued retinal pigment

136 cell degeneration, similar to that of *ent2* RNAi flies.

137 To examine the level of mHTT aggregate formation in the *Drosophila* brain, we

138 drove the expression of transgenes using *elav-GAL4* and stained the brains with mHTT

139 antibody (MW8), which exclusively stains mHTT inclusions (Ko et al., 2001). The

140 results showed that mHTT inclusions were reduced to 50% in 10-day-old Q93 *adoR*

141 RNAi flies (Fig. 2B&C), with 20-day-old Q93 *adoR* RNAi flies exhibiting a similar level

142 of suppression (Fig. S4). Our results demonstrate that decreased e-Ado signaling by

143 either knocking down the transporter *ent2* or *adoR* has a strong influence on reducing

144 mHTT-induced cell cytotoxicity and mHTT aggregate formation.

145

Epistatic interaction of *adoR* and *ent2* on mHTT-induced mortality

The above results indicated that knockdown of *adoR*, *ent1*, or *ent2* expression significantly extended the adult longevity of mHTT files (Fig. 1E). Therefore, we next tested whether there is a synergy between the effects of *adoR* and both transporters. First, we co-expressed *adoR* RNAi constructs with *ent1* RNAi in Q93-expressing flies. As shown in Fig. 3A, the double knockdown of *ent1* and *adoR* shows a sum of individual effects on lifespan which is greater than the knockdown of *adoR* alone. There seems to be a synergy between *ent1* and *adoR*, suggesting that *ent1* may have its own effect which is partially independent from *adoR* signaling. In contrast, when we performed a double knockdown of *adoR* and *ent2* RNAi in Q93-expressing flies, the silencing of both had the same effect as silencing *adoR* only, indicating that they are involved in the same pathway.

Identification of potential downstream targets of the AdoR pathway

Our results indicate that *ent2* and *adoR* modify mHTT cytotoxicity and belong to the same pathway. To identify their potential downstream target genes, we compared the gene expression profiles of larvae carrying mutations in *adoR* or *ent2* as well as adult *adoR* mutants by using microarrays (Affymetrix). The data are presented as Venn diagrams, which show the intersection between differentially-expressed genes for individual mutants in all three data sets, including six upregulated (Fig. 3B) and seven downregulated mRNAs (Fig. 3C). According to Flybase annotations (http://flybase.org), four of these genes were expressed in the nervous system (*ptp99A* was upregulated, while *CG6184*, *cindr*, and *mod(mdg4)* were downregulated) (Tab. S1).

In order to examine the potential roles of these four genes in the interaction with mHTT, we co-expressed RNAi constructs of these candidate genes with mHTT and assessed the adult lifespan (Fig. 3D). The results showed that only the knockdown of *mod(mdg4)* extended the lifespan of mHTT-expressing flies, and that the survival curve was not significantly different from that of *adoR* RNAi Q93 flies. Furthermore, *mod(mdg4)* RNAi

6

174   was the only one of these constructs that significantly reduced retinal pigment cell

175   degeneration (Fig. 3E) and decreased the formation of mHTT inclusions (Fig. 3F&G).

176   We next examined the possible epistatic relationship between *ent2*, *adoR*, and *mod(mdg4)*

177   by combining the overexpression of *ent2* or *adoR* with *mod(mdg4)* RNAi in mHTT-

178   expressing flies (Fig. 3H). The results showed that the knockdown of *mod(mdg4)* RNAi

179   was able to minimize the lethal effects caused by *ent2* and *adoR* overexpression in mHTT

180   flies. This indicated that *mod(mdg4)* is a downstream target of the AdoR pathway. In

181   addition, we found that increasing the e-Ado concentration by microinjecting Ado

182   significantly increased *mod(mdg4)* expression in GAL4 control flies but not in the flies

183   with *adoR* knockdown (Fig. 3I). *mod(mdg4)* expression in the brain of mHTT Q93 larvae

184   was lower than in control Q20 HTT larvae (Fig. 3J). This result is consistent with a lower

185   e-Ado level in Q93 mHTT larvae (Fig. 1A).

186   Taken together, our results demonstrate that *mod(mdg4)* serves as a major downstream

187   target of the AdoR pathway, modulating the process of mHTT inclusion formation and

188   mHTT-induced cytotoxicity.

189   **AdoR pathway with Mod(mdg4) as regulators of Hsp70 protein production**

190   Earlier studies on *Drosophila* protein two-hybrid screening have indicated that

191   Mod(mdg4) is able to interact with six proteins from the Hsp70 family (Giot et al.,

192   2003;Oughtred et al., 2019). In addition, Hsp70 family proteins are known to contribute

193   to suppressing mHTT aggregate formation (Warrick et al., 1999;Chan et al., 2000). In the

194   present study, we compared the levels of Hsp70 protein in *adoR* and *mod(mdg4)* RNAi

195   flies (Figs. 4A, 4B and S5); the results showed that both knockdowns doubled the level of

196   Hsp70 compared to *elav-Gal4* control flies under a non-stress condition (i.e. without

197   mHTT expression). We next compared the level of Hsp70 in flies co-expressing mHTT

198   with each RNAi construct (Figs 4C, 4D and S6). Interestingly, both *adoR* and *mod(mdg4)*

199   RNAi flies co-expressing Q93 mHTT again showed levels around two-fold higher than

200   the Q20 HTT-expressing control, although it was around ten times higher in Q93 mHTT-

201   only flies. These results indicate that *adoR* and *mod(mdg4)* are able to suppress Hsp70

202   protein production under a non-stress condition. The knockdown of *adoR* and *mod(mdg4)*

203 leads to an increase of Hsp70 production, thus preventing mHTT aggregate formation

204 and decreasing mHTT cytotoxicity.

205

206 **Decreased susceptibility to oxidative and heat-shock stresses in *adoR* mutant flies**

207 Since Hsp70 proteins are also involved in the response against oxidative stress (Azad et

208 al., 2011;Shukla et al., 2014;Donovan and Marr, 2016) and heat-shock stress (Gong and

209 Golic, 2006;Bettencourt et al., 2008;Shilova et al., 2018) in *Drosophila*, we postulated

210 that increased Hsp70 production by decreased e-Ado signaling may also enhance the

211 resistance against both stresses. To test this, we treated flies with either paraquat (a potent

212 oxidative stress inducer; Fig. 4E) or a higher temperature (to induce heat-shock; Fig. 4F).

213 We then compared the survival rate between the mutant flies and w[1118] or Canton-S

214 control flies. The results showed that *adoR* mutant flies were more resistant to paraquat

215 and heat-shock treatment. Our results therefore demonstrate that the *Drosophila* AdoR

216 pathway with its downstream gene *mod(mdg4)* suppresses Hsp70 protein production

217 under a non-stress condition. Thus, the knockdown of *ent2*, *AdoR*, and *mod*(*mdg4*) results

218 in increased levels of Hsp70, which in turn helps flies to respond to various stresses,

219 including mHTT cytotoxicity, oxidative and heat-shock stresses (Fig. 4G).

220

221 **Discussion**

222 Ado signaling represents an evolutionarily conserved pathway affecting a diverse

223 array of stress responses (Fredholm, 2007). As a ubiquitous metabolite, Ado has evolved

224 to become a conservative signal among eukaryotes. In previous studies, *Drosophila adoR*

225 mutants (Dolezelova et al., 2007;Wu et al., 2009) and mice with a knockout of all four

226 *adoRs* (Xiao et al., 2019) both displayed minor physiological alteration under normal

227 conditions. This is consistent with the idea that Ado signaling more likely regulates the

228 response to environmental changes (stresses) rather than being involved in maintaining

229 fundamental homeostasis in both insect and mammalian models. Our study examined the

230 impact of altering the expression of genes involved in Ado signaling and metabolism on

231 the cytotoxicity and neurodegeneration phenotype of Q93 mHTT-expressing flies. We

8

232   discovered a novel downstream target of this pathway, *mod(mdg4)*, and showed its
233   effects on the downregulation of Hsp70 proteins, a well-known chaperone responsible for
234   protecting cells against various stress conditions, including mHTT cytotoxicity, as well as
235   thermal or oxidative stress (Soares et al., 2019).

236   The low level of Ado observed in our *da-Gal4* mHTT flies suggests that it might
237   have a physiological role; lowering of the Ado level might represent a physiological
238   response to cytotoxic stress. Consistently, our experimentally-decreased Ado signal
239   rescued the mHTT phenotype, while an increased Ado signal had deleterious effects.
240   Interestingly, a high level of Ado in the hemolymph has previously been observed in
241   *Drosophila* infected by a parasitoid wasp (Novakova and Dolezal, 2011;Bajgar et al.,
242   2015). A raised e-Ado titer has not only been shown to stimulate hemocyte proliferation
243   in the lymph glands (Mondal et al., 2011), but also to trigger metabolic reprogramming
244   and to switch the energy supply towards hemocytes (Bajgar et al., 2015). In contrast, our
245   experiments show that a lowered e-Ado titer results in increased Hsp70 production.
246   Increased Hsp70 has previously been shown to protect the cells from protein aggregates
247   and cytotoxicity caused by mHTT expression, as well as some other challenges including
248   oxidative stress (paraquat treatment) or heat-shock (Garbuz, 2017). The fine regulation of
249   extracellular Ado in *Drosophila* might mediate the differential Ado responses via a single
250   receptor isoform. Our earlier experiments on *Drosophila* cells also suggested that
251   different cell types have different responses to Ado signaling (Fleischmannova et al.,
252   2012).

253   Our data also showed that altered adenosine signaling through the receptor is
254   closely connected to Ado transport, especially to ent2 transporter function. We observed
255   that *adoR* and *ent2* knockdowns provide the most prominent rescue of mHTT phenotypes.
256   In addition, the overexpression of *adoR* and *ent2* genes results in effects that are opposite
257   to their knockdowns, thus supporting the importance of these genes as key regulators of
258   mHTT phenotypes. Our previous report showed that responses to *adoR* and *ent2*
259   mutations cause identical defects in associative learning and synaptic transmission
260   (Knight et al., 2010). In the present study, we show that the phenotypic response of
261   mHTT flies to *adoR* and *ent2* knockdowns are also identical. Our results suggest that the

262 source of e-Ado for inducing AdoR signaling is mainly released by *ent2*. Consistently,

263 the knockdown of *ent2* has previously been shown to block Ado release from *Drosophila*

264 hemocytes upon an immune challenge (Bajgar et al., 2015), as well as from wounded

265 cells stimulated by *scrib*-RNAi (Poernbacher and Vincent, 2018) or bleomycin feeding

266 (Xu et al., 2020). These data support the idea that both *adoR* and *ent2* work in the same

267 signaling pathway.

268   Our results revealed that lower AdoR signaling has a beneficial effect on mHTT-

269 expressing flies, including increasing their tolerance to oxidative and heat-shock stresses.

270 The effect of lower Ado signaling in mammals has been studied by pharmacologically

271 blockading AdoRs, especially by the non-selective adenosine receptor antagonist caffeine.

272 Interestingly, caffeine has beneficial effects on both neurodegenerative diseases and

273 oxidative stress in humans (Rivera-Oliver and Diaz-Rios, 2014;Martini et al., 2016). In

274 contrast, higher long-term Ado concentrations have cytotoxic effects by itself in both

275 insect and mammalian cells (Schrier et al., 2001;Merighi et al., 2002). Chronic exposure

276 to elevated Ado levels has a deleterious effect, causing tissue dysfunction, as has been

277 observed in a mammalian system (Antonioli et al., 2019). Such disruption of nucleotide

278 homeostasis has also been observed in mHTT-expressing R6/2 and Hdh150 mice

279 (Toczek et al., 2016).

280   We identified a downstream target of the AdoR pathway, *mod(mdg4)*, which

281 modulates mHTT cytotoxicity and aggregations. This gene has previously been

282 implicated in the regulation of position effect variegation, chromatin structure, and

283 neurodevelopment (Dorn and Krauss, 2003). The altered expression of *mod(mdg4)* has

284 been observed in flies expressing untranslated RNA containing CAG and CUG repeats

285 (Mutsuddi et al., 2004;van Eyk et al., 2011). In addition, *mod(mdg4)* has complex

286 splicing, including *trans*-splicing, producing at least 31 isoforms (Krauss and Dorn,

287 2004). All isoforms contain a common N-terminal BTB/POZ domain which mediates the

288 formation of homomeric, heteromeric, and oligomeric protein complexes (Bardwell and

289 Treisman, 1994;Albagli et al., 1995;Espinas et al., 1999). Among these isoforms, only

290 two [including *mod(mdg4)*-56.3 (isoform H) and *mod(mdg4)*-67.2 (isoform T)] have been

291 functionally characterized. *mod(mdg4)*-56.3 is required during meiosis for maintaining

292 chromosome pairing and segregation in males (Thomas et al., 2005;Soltani-Bejnood et al.,
293 2007). *mod(mdg4)-67.2* interacts with suppressor of hairy wing [Su(Hw)] and
294 Centrosomal protein 190 kD (CP190) forming a chromatin insulator complex which
295 inhibits the action of the enhancer on the promoter, and is important for early embryo
296 development and oogenesis (Buchner et al., 2000;Soshnev et al., 2013;Melnikova et al.,
297 2018). In the present study, we showed that *mod(mdg4)* is controlled by AdoR which
298 consecutively works as a suppressor of Hsp70 chaperone. The downregulation of *adoR* or
299 *mod(mdg4)* leads to the induction of Hsp70, which in turn suppresses mHTT aggregate
300 formation and other stress phenotypes. Although our results showed that silencing all
301 *mod(mdg4)* isoforms decreases cytotoxicity and mHTT inclusion formation, we could not
302 clarify which of the specific isoforms is involved in such effects, since AdoR seems to
303 regulate the transcriptions of multiple isoforms (Fig. S7). Further study will be needed to
304 identify the specific *mod(mdg4)* isoform(s) connected to Hsp70 production.

305   In summary, our data suggest that the cascade (*ent2*)-*AdoR-mod(mdg4)-Hsp70*
306 might represent an important general Ado signaling pathway involved in the response to
307 various stress conditions, including reaction to mHTT cytotoxicity, oxidative damage, or
308 thermal stress in *Drosophila* cells. The present study provides important insights into the
309 molecular mechanisms of how Ado regulates mHTT aggregate formation and stress
310 responses in *Drosophila*; this might be broadly applicable for understanding how the
311 action of Ado affects disease pathogenesis.

Materials and methods

Fly stocks

Flies were reared at 25 ℃ on standard cornmeal medium. The following RNAi lines were acquired from the TRiP collection (Transgenic RNAi project) at Harvard Medical School: adgfA-Ri (BL67233), adgfC-Ri (BL42915), adgfD-Ri (BL56980), adenoK-Ri (BL64491), ent1-Ri (BL51055), adoR-Ri (BL27536), gfp-Ri (BL41552), mod(mdg4)-Ri (BL32995), cindr-Ri (BL38976), and ptp99A-Ri (BL57299). The following RNAi lines were acquired from the Vienna Drosophila RNAi Center (VDRC): ent2-Ri (ID100464), ent3-Ri (ID47536), cnt2-Ri (ID37161), and cg6184-Ri (ID107150).

Flies overexpressing human normal huntingtin (HTT) exon 1, Q20Httexon[1111F1L], mutant pathogenic fragments (mHTT), Q93Httexon[14F132] and elav[C155]-GAL4 were obtained from Prof. Lawrence Marsh (UC Irvine, USA) (Steffan et al., 2001). The UAS-overexpression lines, Ox-adenoK and Ox-adoR, were obtained from Dr. Ingrid Poernbacher (The Francis Crick Institute, UK) (Poernbacher and Vincent, 2018). gmr-GAL4 was obtained from Dr. Marek Jindra (Biology Centre CAS, Czechia). da-GAL4 was obtained from Dr. Ulrich Theopold (Stockholm University). The UAS overexpression strains Ox-adgfA, Ox-ent2, adoR[1] and ent2[3] mutant flies, were generated in our previous studies (Dolezal et al., 2003;Dolezal et al., 2005;Dolezelova et al., 2007;Knight et al., 2010).

Eclosion rate and adult lifespan assay

For assessing the eclosion rate, male flies containing the desired RNAi or overexpression transgene (RiOx) in the second chromosome with genotype w[1118]/Y; RiOx /CyO; UAS-Q93/MKRS were crossed with females of *elav-GAL4*; +/+; +/+. The ratio of eclosed adults between *elav-GAL4*/+; RiOx/+; UAS-Q93/+ and *elav-GAL4*/+; RiOx/+; +/MKRS was then calculated. If the desired RiOx transgene was in the third chromosome, female flies containing *elav-GAL4*; +/+; RiOx were crossed with male w[1118]/Y; +/+; UAS-Q93/MKRS, and the ratio of eclosed adults between *elav-GAL4*; +/+; RiOx/UAS-Q93 and *elav-GAL4*; +/+; RiOx/MKRS was calculated.

For the adult survival assay, up to 30 newly-emerged female adults were placed in each cornmeal-containing vial and maintained at 25 ℃. At least 200 flies of each

342   genotype were tested and the number of dead flies was counted every day. Flies co-

343   expressing RiOx and HTT Q20 were used for evaluating the effect of RNAi or

344   overexpression of the desired transgenes.

345

346   **Extracellular adenosine and ATP level measurements**

347   To collect the hemolymph, 6 third-instar larvae (96 hours post-oviposition) were torn in

348   150 µl of 1× PBS containing thiourea (0.1 mg/ml) to prevent melanization. The samples

349   were then centrifuged at 5000× g for 5 min to separate the hemocytes and the supernatant

350   was collected for measuring the extracellular adenosine or ATP level. For measuring the

351   adenosine titer, 10 µl of hemolymph was mixed with the reagents of an adenosine assay

352   kit (Biovision) following the manufacturer's instructions. The fluorescent intensity was

353   then quantified (Ex/Em = 533/587 nm) using a microplate reader (BioTek Synergy 4).

354   For measuring the ATP level, 10 µl of hemolymph was incubated with 50 µl of CellTiter-

355   Glo reagent (Promega) for 10 min. Then, the luminescent intensity was quantified using

356   an Orion II microplate luminometer (Berthold). To calibrate the standard curve of ATP

357   concentration, 25 μM ATP standard solution (Epicentre) was used for preparing a

358   concentration gradient (0, 2, 4, 6, 8, 10 μM) of ATP solution and the luminescent

359   intensity was measured for each concentration. The protein concentration of the

360   hemolymph sample was determined by a Bradford assay. The adenosine and ATP

361   concentrations were first normalized to protein concentration. Then, the values of Q20

362   and Q93 samples were normalized to values of the *GAL4* control sample. Six independent

363   replicates for each genotype were performed for the analysis of adenosine and ATP levels.

364

365   **RNA extraction**

366   The brains of 10 third-instar larvae (96 hours post-oviposition) or 15 whole female flies

367   were pooled for each replicate. The samples were first homogenized in RiboZol (VWR)

368   and the RNA phase was separated by chloroform. For brain samples, the RNA was

369   precipitated by isopropanol, washed in 75% ethanol, and dissolved in nuclease-free water.

370   For whole fly samples, the RNA phase was purified using NucleoSpin RNA columns

371   (Macherey-Nagel) following the manufacturer's instructions. All purified RNA samples

13

372   were treated with DNase to prevent genomic DNA contamination. cDNA was

373   synthesized from 2 µg of total RNA using a RevertAid H Minus First Strand cDNA

374   Synthesis Kit (Thermo Fisher Scientific).

375   **Adenosine injection**

376   Three- to five-day-old female adults were injected with 50 nl of 10 mM adenosine

377   solution using a NANOJECT II (Drummond Scientific); control flies were injected with

378   50 nl of 1× PBS. Two hours post-injection, 15 injected flies for each replicate were

379   collected for RNA extraction.

380   **Microarray analysis**

381   The Affymetrix GeneChip® *Drosophila* genome 2.0 array system was used for

382   microarray analysis following the standard protocol: 100 ng of RNA was amplified with

383   a GeneChip 3′ express kit (Affymetrix), and 10 µg of labeled cRNA was hybridized to the

384   chip according to the manufacturer's instructions. The statistical analysis of array data

385   was as described in our previous studies (Arefin et al., 2014;Kucerova et al., 2016).

386   Storey's q value (false discovery rate, FDR) was used to select significantly differentially

387   transcribed genes (q < 0.05). Transcription raw data are shown in Table S2 and have been

388   deposited in the ArrayExpress database (www.ebi.ac.uk/arrayexpress; accession No. E-

389   MTAB-8699 and E-MTAB-8704).

390

391   **qPCR and primers**

392

393   5× HOT FIREPol® EvaGreen® qPCR Mix Plus with ROX (Solis Biodyne) and an Eco

394   Real-Time PCR System (Illumina) were used for qPCR. Each reaction contained 4 µl of

395   EvaGreen qPCR mix, 0.5 µl each of forward and reverse primers (10 µM), 5 µl of diluted

396   cDNA, and ddH2O to adjust the total volume to 20 µl. The list of primers is shown in

397   Table S3. The expression level was calculated using the $2^{-\Delta\Delta Ct}$ method with the ct values

398   of target genes normalized to a reference gene, ribosomal protein 49 (*rp49*).

399

400   **Imaging of retinal pigment cell degeneration**

401 Twenty- and thirty-day-old female adults were collected and their eye depigmentation

402 phenotypes were recorded. At least 30 individuals for each genotype were examined

403 under a microscope, and at least five representative individuals were chosen for imaging.

404 Pictures were taken with an EOS 550D camera (Canon) mounted on a SteREO Discovery

405 V8 microscope (Zeiss).

Brain immunostaining

407 Brains dissected from 10- or 20-day-old adult females were used for immunostaining.

408 The brains were fixed in 4% PFA, permeabilized with PBST (0.1% Triton X-100),

409 blocked in PAT (PBS, 0.1% Triton X-100, 1% BSA) and stained with antibodies in PBT

410 (PBS, 0.3% Triton X-100, 0.1% BSA). Primary antibodies used in this study were mouse

411 anti-HTT; MW8, which specifically binds to mHTT aggregates (1:40, DSHB); and rat

412 anti-Elav (1:40, DSHB), which is a pan-neuronal antibody. Secondary antibodies were

413 Alexa Fluor 488 anti-mouse and Alexa Fluor 647 anti-rat (1:200, Invitrogen). The

414 samples were mounted in Fluoromount-G (Thermo Fisher Scientific) overnight, prior to

415 image examination.

416

417 **Quantification of mHTT aggregates**

418 Images of aggregates were taken using a FluoView 100 confocal microscope (Olympus).

419 The intensity of mHTT aggregates detected by anti-HTT antibody (MW8) or anti-Elav

420 were quantified using ImageJ software. The level of mHTT aggregates was quantified by

421 normalizing the covering area of mHTT aggregate signal to Elav signal. At least six brain

422 images from each genotype were analyzed.

423

424 **Western blot**

425 Twenty heads, collected from 10-day-old adult females, were pooled for each replicate.

426 The samples were homogenized in 100 μl of RIPA buffer with 1 μl of Halt™ proteinase

427 inhibitor cocktail (Thermo Fisher Scientific). From each sample, 80 μl of supernatant was

428 collected after 10 min of centrifugation at $12000 \times g$, which was then mixed with 16 μl of

429 $6\times$ loading buffer. After boiling at 95 °C for 3 min, 10 μl were then loaded for running an

430 SDS-PAGE gel. Proteins were then transfered to an Immobilon-E PVDF membrane

431 (Millipore), which was then washed with 1× PBS containing 0.05% Tween 20 (three

432 washes, each 15 min) and blocked in 5% BSA for 1 hour at room temperature before

433 staining. The membrane was subsequently stained with primary antibodies overnight at 4

434 °C and secondary antibody for 1 hour at room temperature. After immunostaining, the

435 membrane was treated with 2 ml of SuperSignal™ West Pico PLUS Chemiluminescent

436 Substrate (Thermo Fisher Scientific) for 10 min at room temperature, and images were

437 recorded using a Fujifilm LAS-3000 Imager. The primary antibodies used for staining

438 were rat anti-Hsp70(7FB) (1:2000, Thermo Fisher Scientific) and mouse anti-Tub (1:500,

439 DSHB). The secondary antibodies were donkey anti-rat IgG (H+L) HRP (1:5000,

440 Thermo Fisher Scientific) and donkey anti-Mouse IgG (H+L) HRP (1:5000, Thermo

441 Fisher Scientific).

442

443 Paraquat injection

444 Three- to five-day-old males were collected for paraquat injection. Each fly was injected

445 with 50 nl of 3 mM paraquat ringer solution using a NANOJECT II (Drummond

446 Scientific). Control flies were injected with ringer buffer. Seventeen to twenty of injected

447 flies were pooled into one vial for each replicate, and six replicates were performed for

448 each treatment.

449

450 Heat-shock treatment

451 The heat-shock procedure followed a previous study (Gong and Golic, 2006) with few

452 modifications. Newly emerged males (0 or 1 day old) were collected and maintained on a

453 standard cornmeal diet. The following day, ten flies were transferred into each empty vial

454 and given a mild heat-shock at 35 °C for 30 min, then transferred to a circulating water

455 bath at 39 °C. The number of surviving flies was checked every 10 min; flies which did

456 not move any part of their body were considered dead.

457

458 Statistical analysis

459 A Shapiro-Wilk test was applied to determine data normality. For data which were not

460 normally distributed ($P < 0.05$), statistical significance was analyzed using the Mann-

461 Whitney U-test. For normally distributed data ($P > 0.05$), statistical significance was

16

462 established using Student's t-test or one-way ANOVA with Tukey's HSD *post-hoc* test.

463 For the statistical analysis of survival curves, we used OASIS 2 to perform a weighted

464 log-rank test (Han et al., 2016).

465

466 **Figures**

Fig. 1

467

468
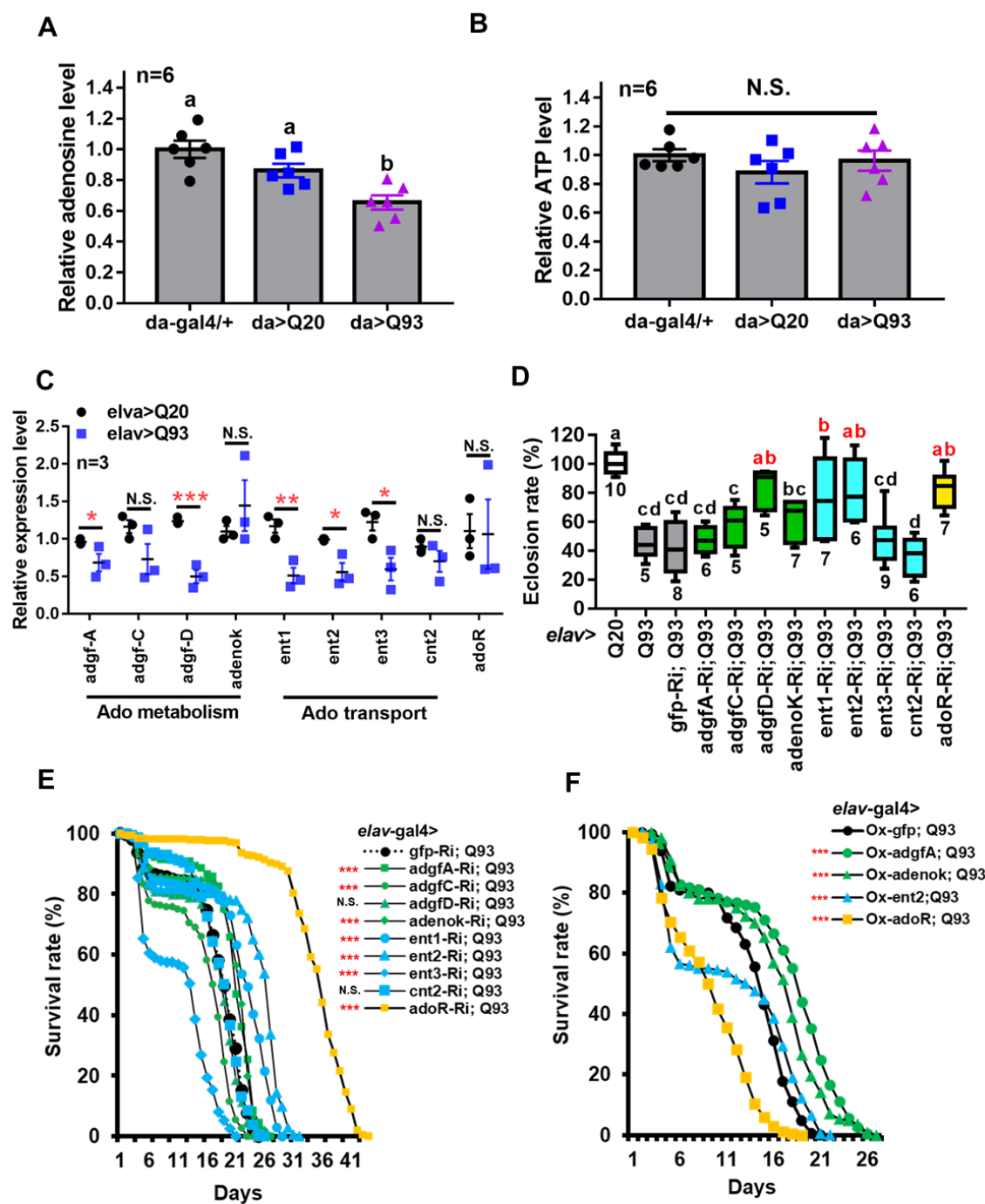
469 **Figure 1 Reduced extracellular Ado transport and receptor suppress mHTT**
470 **induced lethality**

471 (A-B) Relative level of extracellular Ado (A) and ATP (B) titers in Q93-expressing
472 (da>Q93), Q20-expressing (da>Q20), and control *da*-GAL4 (da/+) larvae. Ado and ATP
473 concentration are normalized to control larvae. Significance was analyzed by ANOVA;
474 significant differences ($P < 0.05$) among treatment groups are marked with different
475 letters; N.S., not significant; n = 6. Error bars are presented as mean ± SEM

476 (C) Transcriptions level of genes involved in regulating Ado homeostasis in Q93-
477 expressing (elav>Q93) and control Q20-expressing (elav>Q20) larval brains.
478 Significance was analyzed by Student's t-test and labeled as follows: $*P < 0.05$, $**P <$
479 0.01, $***P < 0.001$; N.S., not significant. n = 3. Error bars are presented as mean ± SEM

480 (D) Eclosion rate of mHTT-expressing adult females (elav>Q93) with RNAi silencing
481 (Ri) Ado metabolic enzymes, transporters, *adoR* and control *gfp*. Numbers below each
482 column indicate the number of replicates (n). Significance was analyzed by ANOVA;
483 significant differences ($P < 0.05$) among treatment groups are marked with different
484 letters

485 (E) Survival of mHTT-expressing adult females (elav>Q93) with RNAi silencing (Ri)
486 Ado metabolic enzymes, transporters, *adoR* and control *gfp*. Significance was analyzed
487 by weighted log-rank test; significant differences between each treatment group and
488 control (*gfp*-Ri) are labeled as follows: $***P < 0.001$; N.S., not significant. n > 200

489 (F) Survival of mHTT-expressing adult females (elav>Q93) overexpressing (Ox) Ado
490 metabolic enzymes (*adgf-A* and *adenok*), transporters (*ent2*), *adoR*, and control *gfp*.
491 Significance was analyzed by a weighted log-rank test; significant differences between
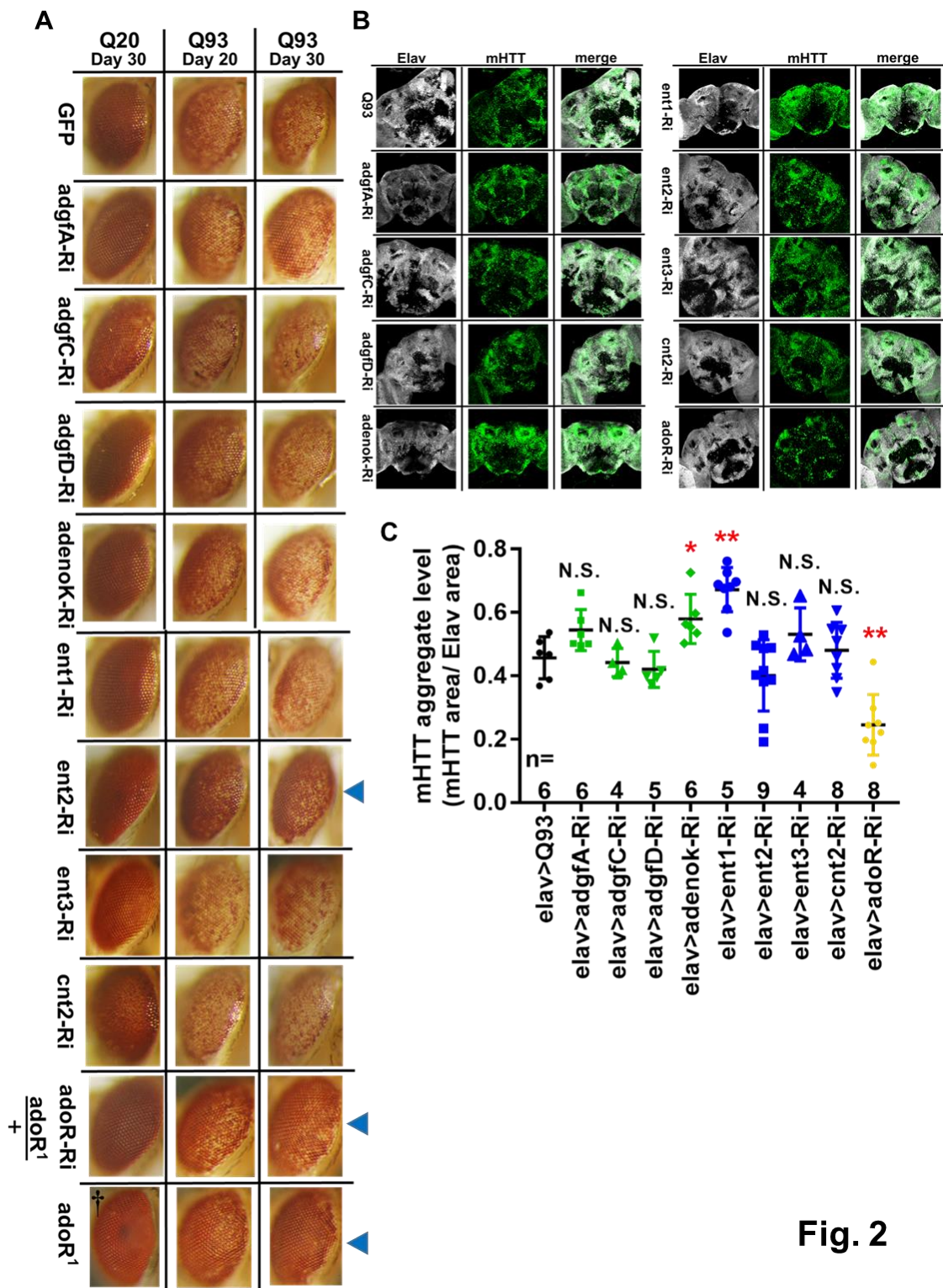492 each treatment group to control (*gfp*-Ri) are labeled as $***P < 0.001$. n > 200
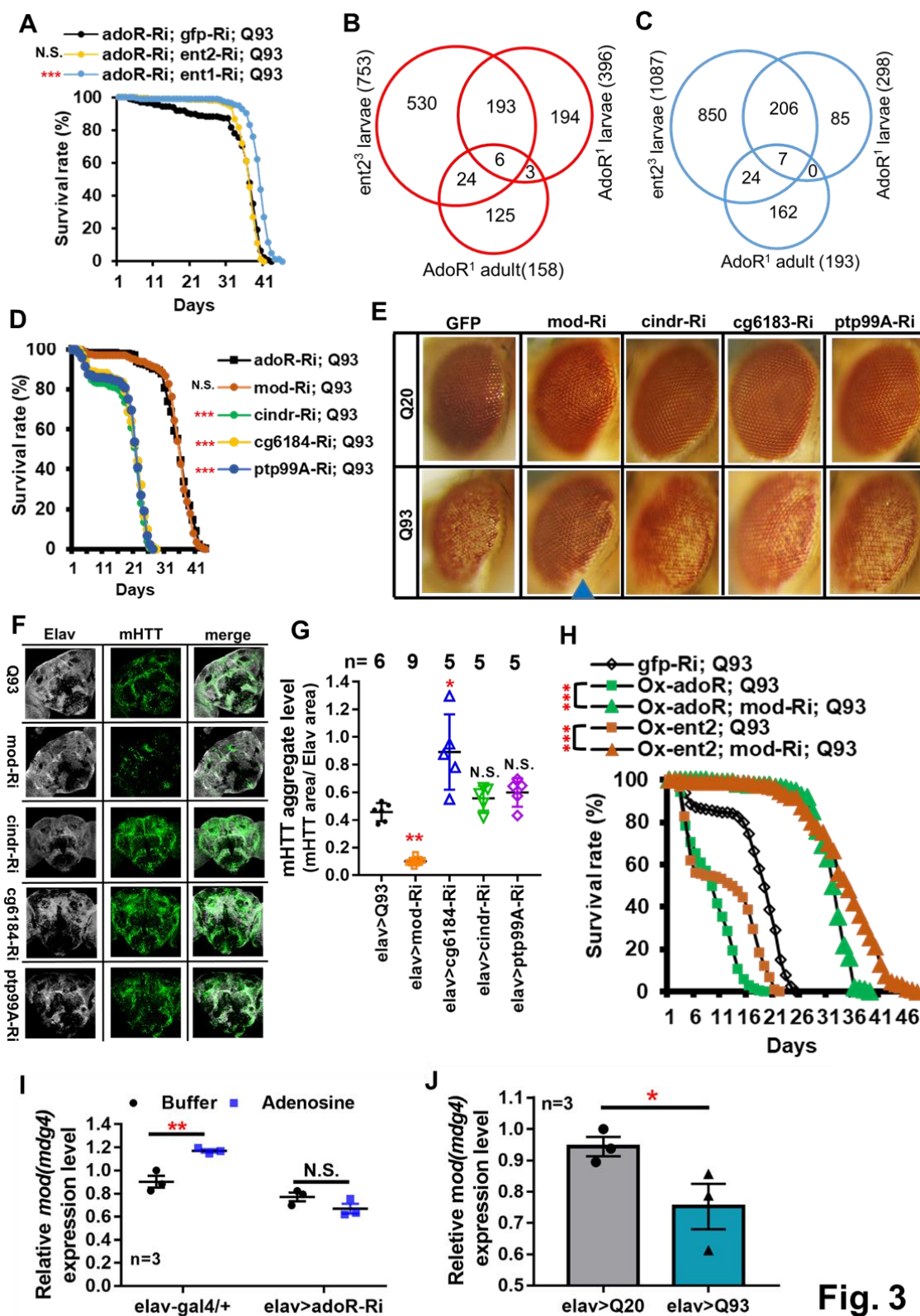
493

494

495

496

Fig. 2

497

498

499 **Figure 2 Suppression of *ent2* and *adoR* decreased mHTT-induced cytotoxicity and**

500 **mHTT aggregate formation**

501 (A) Retinal pigment cell degeneration in mHTT-expressing adult females (gmr>Q93)

502 with RNAi silencing Ado metabolic enzymes, transporters, *adoR* (*adoR* heterozygous

503 mutant background) and mHTT-expressing flies under *adoR* homozygous mutant

504 background. Blue arrows indicate treated groups showing a significantly reduced loss of

505 pigment. †Eye image of control homozygous *adoR^1* mutant without *htt* expression.

506 Detailed methodologies for sample collection and eye imaging are described in Materials

507 and methods

508 (B) Representative confocal images of the brains of 10-day-old mHTT-expressing adult

509 females (elav>Q93) with RNAi silencing Ado metabolic enzymes, transporters, and *adoR*.

510 Neuronal cells were detected with anti-Elav; mHTT aggregates were detected with anti-

511 HTT (MW8)

512 (C) Level of mHTT aggregation formation was calculated by normalizing the area of

513 mHTT signal to the area of Elav signal. Significance in mHTT aggregate levels was

514 analyzed using a Mann-Whitney U-test; significant differences between control Q93 flies

515 and each RNAi treatment group are labeled as follows: *$P < 0.05$; **$P < 0.01$; N.S., not

516 significant. Error bars are presented as mean ± SEM. The number (n) of examined brain

517 images are shown below each bar

518

519

520

521

522

523

524

525

Fig. 3

526

527

Figure 3 Mod(mdg4) as a downstream target of ENT2/AdoR pathway modulated mHTT effects and aggregate formation

(A) Survival of mHTT-expressing adult females (elav>Q93) with RNAi co-silencing (Ri) transporters (*ent1* or *ent2*) and *adoR*. Significance was analyzed by a weighted log-rank test; significant differences between each treatment group and control (*gfp*-Ri) are labeled as follows: ***$P < 0.001$; N.S., not significant. n > 200

(B-C) Microarray analysis of the transcriptomes of *ent2* and *adoR* mutants. Venn diagram shows the number of common genes (in intersect region) which were upregulated (B) or downregulated (C) among the *adoR* mutant larvae vs. control (w^{1118}), *adoR* mutant adults vs. control (w^{1118}), and ent2 mutant larvae vs. control (w^{1118}). The cutoff values for expression differences were set at $Q < 0.05$ (false discovery rate, FDR)

(D) Survival of mHTT-expressing adult females (elav>Q93) with RNAi co-silencing (Ri) of potential downstream genes of the ENT2/AdoR pathway. Significance was analyzed by a weighted log-rank test; significant differences between each treatment group to control (*adoR*-Ri) are labeled as follows: ***$P < 0.001$; N.S., not significant. n > 200

(E) Retinal pigment cell degeneration in mHTT-expressing adult females (gmr>Q93) with RNAi silencing potential downstream genes of the ENT2/AdoR pathway. Blue arrows indicate treated groups showing a significantly reduced loss of pigment. Detailed methodologies for sample collection and eye imaging are described in Materials and methods

(F) Representative confocal images of the brains of 10-day-old mHTT-expressing adult females (elav>Q93) with RNAi silencing potential downstream genes of the ENT2/AdoR pathway. Neuronal cells were detected with anti-Elav and mHTT aggregates were detected with anti-HTT (MW8)

(G) The level of mHTT aggregation formation was calculated by normalizing the area of mHTT signal to the area of Elav signal. Significance in mHTT aggregate levels was analyzed using a Mann-Whitney U-test; significant differences between control Q93 flies and each RNAi treatment group are labeled as follows: *$P < 0.05$; **$P < 0.01$; N.S., not

556   significant. Error bars are presented as mean ± SEM. The number (n) of examined brain

557   images are indicated above each bar

558   (H) Survival of mHTT-expressing adult females (elav>Q93) with co-RNAi silencing

559   *mod(mdg4)* and co-overexpressing *adoR* or *ent2*. Significance was analyzed by a

560   weighted log-rank test; significant differences are labeled as ***$P < 0.001$. n > 200

561   (I) Transcription level of *mod(mdg4)* two hours after Ado injection into the whole body

562   of three- to five-day old control adult females (elav-gal4/+) and *adoR* RNAi females

563   (elav>adoR-Ri). Significance was analyzed by Student's t-test and labeled as follows:

564   **$P < 0.01$; N.S., not significant. n = 3. Error bars are presented as mean ± SEM

565   (J) Transcriptions level of *mod(mdg4)* in Q93-expressing (elav>Q93) and control Q20-

566   expressing (elav>Q20) larval brains. Significance was analyzed by Student's t-test and

567   labeled as *$P < 0.05$. n = 3. Error bars are presented as mean ± SEM

568

569

570

571

572

573

574

575

576

577

578

579

580

Fig. 4

581

25
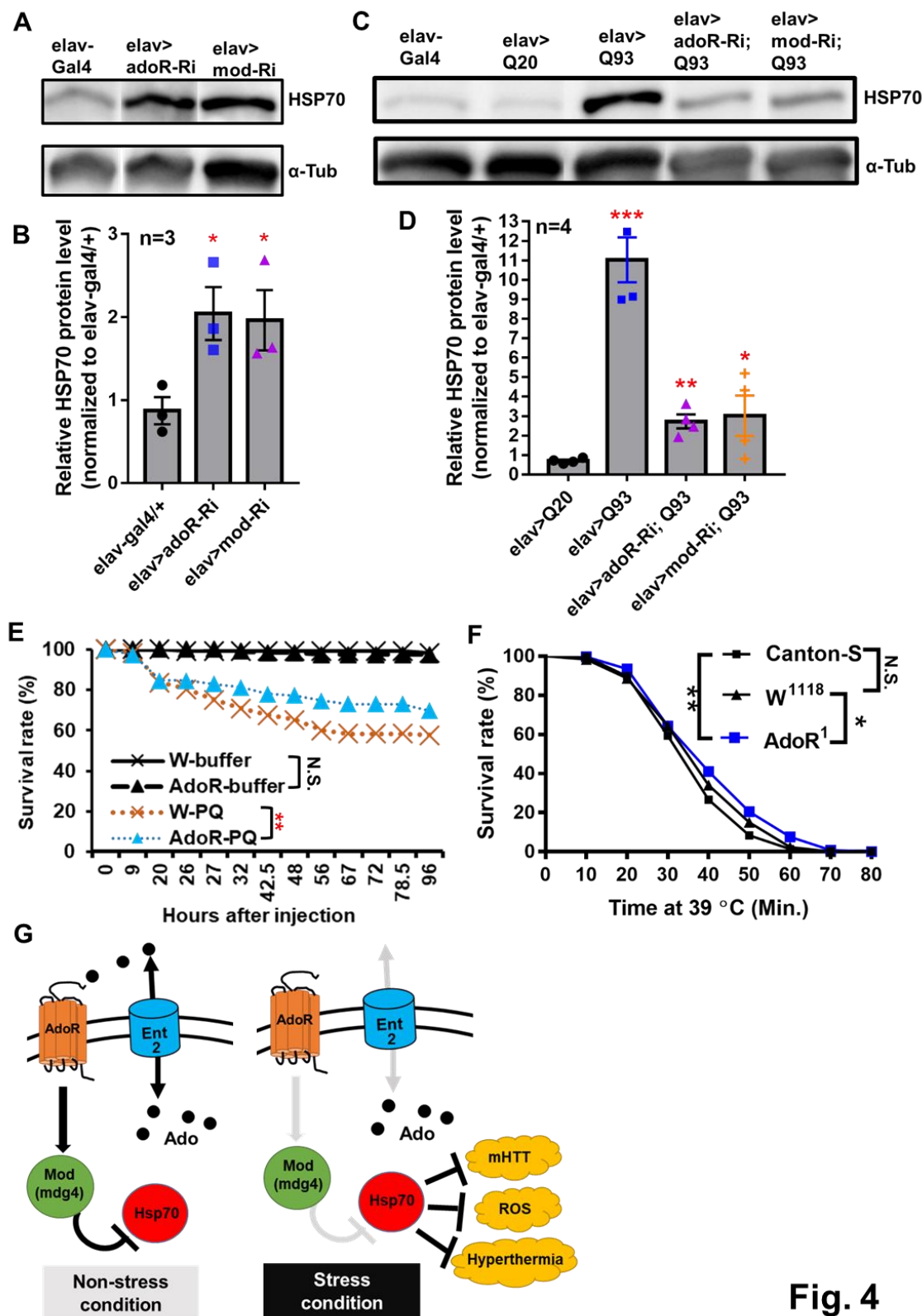
Figure 4 AdoR regulated the Hsp70 protein level and influenced the stress response to paraquat and heat-shock treatments

(A-B) Representative images of western blot analysis. (A) Hsp70 protein level in the head of 10-day-old adult females with RNAi silencing *adoR* (elav>adoR-Ri), *mod(mdg4)* (elav>mod-Ri) and control (elav-gal4/+). (B) The Hsp70 protein level was quantified by normalizing the intensity of the Hsp70 band to the α-Tubulin band using ImageJ; values of RNAi treatment groups were further normalized to the elav-gal4 control. Significance was analyzed by Student's t-test; significant differences between the control and each RNAi treatment group are labeled as *$P < 0.05$. n = 3. Error bars are presented as mean ± SEM. Original gel images are presented in the supplementary materials (Fig. S6)

(C-D) Representative image of western blot analysis. (C) Hsp70 protein level in the head of 10-day-old HTT (elav>Q20) or mHTT expressing (elav>Q93) adult females with RNAi silencing *adoR* and *mod(mdg4)*. (D) The Hsp70 protein level was quantified by normalizing the intensity of the Hsp70 band to the α-Tubulin band by using ImageJ; values of each treatment group were further normalized to the elav-gal4 control. Significance was analyzed by Student's t-test; significant differences between HTT-expressing flies (elav>Q20) and each RNAi treatment of Q93-expressing flies are labeled as follows: *$P < 0.05$, **$P < 0.01$, ***$P < 0.001$. n = 4. Error bars are presented as mean ± SEM. Original gel images are presented in the supplementary materials (Fig. S7)

(E) Survival of w[1118] and homozygous *adoR* mutant adult males after paraquat (PQ) injection. Control groups were injected with ringer buffer. Significance was analyzed by weighted log-rank test; significant differences are labeled as follows: **$P < 0.01$, N.S., not significant. W-ringer, n =116; AdoR[1]-ringer, n = 118; W-PQ, n =118; AdoR[1]-PQ, n = 119.

(F) Survival of Cantons-S, w[1118] and homozygous *adoR* mutant (AdoR[1]) adult males during heat-shock treatment. Significance was analyzed by weighted log-rank test; significant differences are labeled as follows: *$P < 0.05$, **$P < 0.01$. Cantons-S and W[1118], n = 300; AdoR[1], n = 370

26

610 (G) Summary model of Ado signaling under stress response. Under a non-stress
611 condition, the activated AdoR and Mod(mdg4) reduce Hsp70 production. In contrast,
612 decreased Ado signaling under a stress condition resulted in Hsp70 production, which in
613 turn enhanced stress tolerance

614

Acknowledgements

624

Author Contributions

626 Y-HL performed the experiments and prepared the manuscript. HM assisted in recording
627 the adult lifespan and eye phenotypes, and also as performed the brain dissection,
628 immunochemistry and confocal microscopy imaging. LK performed the microarray
629 sample preparation, analyzed the microarray data and paraquat injection. LR assisted in
630 recording the adult lifespan and eye phenotypes, prepared fly strains and performed heat-
631 shock treatment. TF established the methodologies for recording the eclosion rate and
632 survival, and prepared fly strains. MZ conceived the project and supervised manuscript
633 preparation.

634

References

635 Albagli, O., Dhordain, P., Deweindt, C., Lecocq, G., and Leprince, D. (1995). The
636 BTB/POZ domain: a new protein-protein interaction motif common to DNA- and actin-
638 binding proteins. *Cell Growth Differ* 6**,** 1193-1198.

639 Antonioli, L., Fornai, M., Blandizzi, C., Pacher, P., and Hasko, G. (2019). Adenosine
640 signaling and the immune system: When a lot could be too much. *Immunol Lett* 205**,** 9-15.

641 Arefin, B., Kucerova, L., Dobes, P., Markus, R., Strnad, H., Wang, Z., Hyrsl, P., Zurovec,
642 M., and Theopold, U. (2014). Genome-wide transcriptional analysis of Drosophila larvae
643 infected by entomopathogenic nematodes shows involvement of complement, recognition
644 and extracellular matrix proteins. *J Innate Immun* 6**,** 192-204.

645 Azad, P., Ryu, J., and Haddad, G.G. (2011). Distinct role of Hsp70 in Drosophila
646 hemocytes during severe hypoxia. *Free Radic Biol Med* 51**,** 530-538.

647 Bajgar, A., Kucerova, K., Jonatova, L., Tomcala, A., Schneedorferova, I., Okrouhlik, J.,
648 and Dolezal, T. (2015). Extracellular adenosine mediates a systemic metabolic switch
649 during immune response. *PLoS Biol* 13**,** e1002135.

650 Bardwell, V.J., and Treisman, R. (1994). The POZ domain: a conserved protein-protein
651 interaction motif. *Genes Dev* 8**,** 1664-1677.

652 Bettencourt, B.R., Hogan, C.C., Nimali, M., and Drohan, B.W. (2008). Inducible and
653 constitutive heat shock gene expression responds to modification of Hsp70 copy number
654 in Drosophila melanogaster but does not compensate for loss of thermotolerance in
655 Hsp70 null flies. *BMC Biol* 6**,** 5.

656 Borea, P.A., Gessi, S., Merighi, S., and Varani, K. (2016). Adenosine as a Multi-
657 Signalling Guardian Angel in Human Diseases: When, Where and How Does it Exert its
658 Protective Effects? *Trends Pharmacol Sci* 37**,** 419-434.

659 Buchner, K., Roth, P., Schotta, G., Krauss, V., Saumweber, H., Reuter, G., and Dorn, R.
660 (2000). Genetic and molecular complexity of the position effect variegation modifier
661 mod(mdg4) in Drosophila. *Genetics* 155**,** 141-157.

662 Chan, H.Y., Warrick, J.M., Gray-Board, G.L., Paulson, H.L., and Bonini, N.M. (2000).
663 Mechanisms of chaperone suppression of polyglutamine disease: selectivity, synergy and
664 modulation of protein solubility in Drosophila. *Hum Mol Genet* 9**,** 2811-2820.

665 Dolezal, T., Dolezelova, E., Zurovec, M., and Bryant, P.J. (2005). A role for adenosine
666 deaminase in Drosophila larval development. *PLoS Biol* 3**,** e201.

667 Dolezal, T., Gazi, M., Zurovec, M., and Bryant, P.J. (2003). Genetic analysis of the
668 ADGF multigene family by homologous recombination and gene conversion in
669 Drosophila. *Genetics* 165**,** 653-666.

28

670 Dolezelova, E., Nothacker, H.P., Civelli, O., Bryant, P.J., and Zurovec, M. (2007). A
671 Drosophila adenosine receptor activates cAMP and calcium signaling. *Insect Biochem*
672 *Mol Biol* 37, 318-329.

673 Dolezelova, E., Zurovec, M., Dolezal, T., Simek, P., and Bryant, P.J. (2005). The
674 emerging role of adenosine deaminases in insects. *Insect Biochem Mol Biol* 35, 381-389.

675 Donovan, M.R., and Marr, M.T., 2nd (2016). dFOXO Activates Large and Small Heat
676 Shock Protein Genes in Response to Oxidative Stress to Maintain Proteostasis in
677 Drosophila. *J Biol Chem* 291, 19042-19050.

678 Dorn, R., and Krauss, V. (2003). The modifier of mdg4 locus in Drosophila: functional
679 complexity is resolved by trans splicing. *Genetica* 117, 165-177.

680 Espinas, M.L., Jimenez-Garcia, E., Vaquero, A., Canudas, S., Bernues, J., and Azorin, F.
681 (1999). The N-terminal POZ domain of GAGA mediates the formation of oligomers that
682 bind DNA with high affinity and specificity. *J Biol Chem* 274, 16461-16469.

683 Fleischmannova, J., Kucerova, L., Sandova, K., Steinbauerova, V., Broz, V., Simek, P.,
684 and Zurovec, M. (2012). Differential response of Drosophila cell lines to extracellular
685 adenosine. *Insect Biochem Mol Biol* 42, 321-331.

686 Fredholm, B.B. (2007). Adenosine, an endogenous distress signal, modulates tissue
687 damage and repair. *Cell Death Differ* 14, 1315-1323.

688 Garbuz, D.G. (2017). Regulation of heat shock gene expression in response to stress.
689 *Molecular Biology* 51, 352-367.

690 Giot, L., Bader, J.S., Brouwer, C., Chaudhuri, A., Kuang, B., Li, Y., Hao, Y.L., Ooi, C.E.,
691 Godwin, B., Vitols, E., Vijayadamodar, G., Pochart, P., Machineni, H., Welsh, M., Kong,
692 Y., Zerhusen, B., Malcolm, R., Varrone, Z., Collis, A., Minto, M., Burgess, S., Mcdaniel,
693 L., Stimpson, E., Spriggs, F., Williams, J., Neurath, K., Ioime, N., Agee, M., Voss, E.,
694 Furtak, K., Renzulli, R., Aanensen, N., Carrolla, S., Bickelhaupt, E., Lazovatsky, Y.,
695 Dasilva, A., Zhong, J., Stanyon, C.A., Finley, R.L., Jr., White, K.P., Braverman, M.,
696 Jarvie, T., Gold, S., Leach, M., Knight, J., Shimkets, R.A., Mckenna, M.P., Chant, J., and
697 Rothberg, J.M. (2003). A protein interaction map of Drosophila melanogaster. *Science*
698 302, 1727-1736.

699 Gong, W.J., and Golic, K.G. (2006). Loss of Hsp70 in Drosophila is pleiotropic, with
700 effects on thermotolerance, recovery from heat shock and neurodegeneration. *Genetics*
701 172, 275-286.

702 Han, S.K., Lee, D., Lee, H., Kim, D., Son, H.G., Yang, J.S., Lee, S.V., and Kim, S.
703 (2016). OASIS 2: online application for survival analysis 2 with features for the analysis
704 of maximal lifespan and healthspan in aging research. *Oncotarget* 7, 56147-56152.

705 Knight, D., Harvey, P.J., Iliadi, K.G., Klose, M.K., Iliadi, N., Dolezelova, E., Charlton,
706 M.P., Zurovec, M., and Boulianne, G.L. (2010). Equilibrative nucleoside transporter 2

707 regulates associative learning and synaptic function in Drosophila. *J Neurosci* 30, 5047-
708 5057.

709 Ko, J., Ou, S., and Patterson, P.H. (2001). New anti-huntingtin monoclonal antibodies:
710 implications for huntingtin conformation and its binding proteins. *Brain Res Bull* 56, 319-
711 329.

712 Krauss, V., and Dorn, R. (2004). Evolution of the trans-splicing Drosophila locus
713 mod(mdg4) in several species of Diptera and Lepidoptera. *Gene* 331, 165-176.

714 Kucerova, L., Broz, V., Arefin, B., Maaroufi, H.O., Hurychova, J., Strnad, H., Zurovec,
715 M., and Theopold, U. (2016). The Drosophila Chitinase-Like Protein IDGF3 Is Involved
716 in Protection against Nematodes and in Wound Healing. *J Innate Immun* 8, 199-210.

717 Kuo, Y., Ren, S., Lao, U., Edgar, B.A., and Wang, T. (2013). Suppression of
718 polyglutamine protein toxicity by co-expression of a heat-shock protein 40 and a heat-
719 shock protein 110. *Cell Death Dis* 4, e833.

720 Lin, Y.H., Maaroufi, H.O., Ibrahim, E., Kucerova, L., and Zurovec, M. (2019).
721 Expression of Human Mutant Huntingtin Protein in Drosophila Hemocytes Impairs
722 Immune Responses. *Front Immunol* 10, 2405.

723 Maier, S.A., Galellis, J.R., and Mcdermid, H.E. (2005). Phylogenetic analysis reveals a
724 novel protein family closely related to adenosine deaminase. *J Mol Evol* 61, 776-794.

725 Marsh, J.L., Walker, H., Theisen, H., Zhu, Y.-Z., Fielder, T., Purcell, J., and Thompson,
726 L.M. (2000). Expanded polyglutamine peptides alone are intrinsically cytotoxic and
727 cause neurodegeneration in Drosophila. *Human Molecular Genetics* 9, 13-25.

728 Martini, D., Del Bo, C., Tassotti, M., Riso, P., Del Rio, D., Brighenti, F., and Porrini, M.
729 (2016). Coffee Consumption and Oxidative Stress: A Review of Human Intervention
730 Studies. *Molecules* 21.

731 Melnikova, L., Kostyuchenko, M., Parshikov, A., Georgiev, P., and Golovnin, A. (2018).
732 Role of Su(Hw) zinc finger 10 and interaction with CP190 and Mod(mdg4) proteins in
733 recruiting the Su(Hw) complex to chromatin sites in Drosophila. *PLoS One* 13, e0193497.

734 Merighi, S., Mirandola, P., Milani, D., Varani, K., Gessi, S., Klotz, K.N., Leung, E.,
735 Baraldi, P.G., and Borea, P.A. (2002). Adenosine receptors as mediators of both cell
736 proliferation and cell death of cultured human melanoma cells. *J Invest Dermatol* 119,
737 923-933.

738 Mondal, B.C., Mukherjee, T., Mandal, L., Evans, C.J., Sinenko, S.A., Martinez-Agosto,
739 J.A., and Banerjee, U. (2011). Interaction between differentiating cell- and niche-derived
740 signals in hematopoietic progenitor maintenance. *Cell* 147, 1589-1600.

741 Moser, G.H., Schrader, J., and Deussen, A. (1989). Turnover of adenosine in plasma of
742 human and dog blood. *Am J Physiol* 256, C799-806.

743 Mugat, B., Parmentier, M.L., Bonneaud, N., Chan, H.Y., and Maschat, F. (2008).
744 Protective role of Engrailed in a Drosophila model of Huntington's disease. *Hum Mol*
745 *Genet* 17**,** 3601-3616.

746 Mutsuddi, M., Marshall, C.M., Benzow, K.A., Koob, M.D., and Rebay, I. (2004). The
747 spinocerebellar ataxia 8 noncoding RNA causes neurodegeneration and associates with
748 staufen in Drosophila. *Curr Biol* 14**,** 302-308.

749 Novakova, M., and Dolezal, T. (2011). Expression of Drosophila adenosine deaminase in
750 immune cells during inflammatory response. *PLoS One* 6**,** e17741.

751 Oughtred, R., Stark, C., Breitkreutz, B.J., Rust, J., Boucher, L., Chang, C., Kolas, N.,
752 O'donnell, L., Leung, G., Mcadam, R., Zhang, F., Dolma, S., Willems, A., Coulombe-
753 Huntington, J., Chatr-Aryamontri, A., Dolinski, K., and Tyers, M. (2019). The BioGRID
754 interaction database: 2019 update. *Nucleic Acids Res* 47**,** D529-D541.

755 Picano, E., and Abbracchio, M.P. (2000). Adenosine, the imperfect endogenous anti-
756 ischemic cardio-neuroprotector. *Brain Res Bull* 52**,** 75-82.

757 Poernbacher, I., and Vincent, J.P. (2018). Epithelial cells release adenosine to promote
758 local TNF production in response to polarity disruption. *Nat Commun* 9**,** 4675.

759 Rivera-Oliver, M., and Diaz-Rios, M. (2014). Using caffeine and other adenosine
760 receptor antagonists and agonists as therapeutic tools against neurodegenerative diseases:
761 a review. *Life Sci* 101**,** 1-9.

762 Rosas-Arellano, A., Estrada-Mondragon, A., Pina, R., Mantellero, C.A., and Castro, M.A.
763 (2018). The Tiny Drosophila Melanogaster for the Biggest Answers in Huntington's
764 Disease. *Int J Mol Sci* 19.

765 Schrier, S.M., Van Tilburg, E.W., Van Der Meulen, H., Ijzerman, A.P., Mulder, G.J., and
766 Nagelkerke, J.F. (2001). Extracellular adenosine-induced apoptosis in mouse
767 neuroblastoma cells: studies on involvement of adenosine receptors and adenosine uptake.
768 *Biochem Pharmacol* 61**,** 417-425.

769 Shilova, V.Y., Zatsepina, O.G., Garbuz, D.G., Funikov, S.Y., Zelentsova, E.S., Schostak,
770 N.G., Kulikov, A.M., and Evgen'ev, M.B. (2018). Heat shock protein 70 from a
771 thermotolerant Diptera species provides higher thermoresistance to Drosophila larvae
772 than correspondent endogenous gene. *Insect Mol Biol* 27**,** 61-72.

773 Shukla, A.K., Pragya, P., Chaouhan, H.S., Tiwari, A.K., Patel, D.K., Abdin, M.Z., and
774 Chowdhuri, D.K. (2014). Heat shock protein-70 (Hsp-70) suppresses paraquat-induced
775 neurodegeneration by inhibiting JNK and caspase-3 activation in Drosophila model of
776 Parkinson's disease. *PLoS One* 9**,** e98886.

777 Soares, T.R., Reis, S.D., Pinho, B.R., Duchen, M.R., and Oliveira, J.M.A. (2019).
778 Targeting the proteostasis network in Huntington's disease. *Ageing Res Rev* 49**,** 92-103.

779   Soltani-Bejnood, M., Thomas, S.E., Villeneuve, L., Schwartz, K., Hong, C.S., and Mckee,
780   B.D. (2007). Role of the mod(mdg4) common region in homolog segregation in
781   Drosophila male meiosis. *Genetics* 176**,** 161-180.

782   Song, W., Smith, M.R., Syed, A., Lukacsovich, T., Barbaro, B.A., Purcell, J., Bornemann,
783   D.J., Burke, J., and Marsh, J.L. (2013). Morphometric analysis of Huntington's disease
784   neurodegeneration in Drosophila. *Methods Mol Biol* 1017**,** 41-57.

785   Soshnev, A.A., Baxley, R.M., Manak, J.R., Tan, K., and Geyer, P.K. (2013). The
786   insulator protein Suppressor of Hairy-wing is an essential transcriptional repressor in the
787   Drosophila ovary. *Development* 140**,** 3613-3623.

788   Steffan, J.S., Bodai, L., Pallos, J., Poelman, M., Mccampbell, A., Apostol, B.L.,
789   Kazantsev, A., Schmidt, E., Zhu, Y.Z., Greenwald, M., Kurokawa, R., Housman, D.E.,
790   Jackson, G.R., Marsh, J.L., and Thompson, L.M. (2001). Histone deacetylase inhibitors
791   arrest polyglutamine-dependent neurodegeneration in Drosophila. *Nature* 413**,** 739-743.

792   Stenesen, D., Suh, J.M., Seo, J., Yu, K., Lee, K.S., Kim, J.S., Min, K.J., and Graff, J.M.
793   (2013). Adenosine nucleotide biosynthesis and AMPK regulate adult life span and
794   mediate the longevity benefit of caloric restriction in flies. *Cell Metab* 17**,** 101-112.

795   Thomas, S.E., Soltani-Bejnood, M., Roth, P., Dorn, R., Logsdon, J.M., Jr., and Mckee,
796   B.D. (2005). Identification of two proteins required for conjunction and regular
797   segregation of achiasmate homologs in Drosophila male meiosis. *Cell* 123**,** 555-568.

798   Toczek, M., Zielonka, D., Zukowska, P., Marcinkowski, J.T., Slominska, E., Isalan, M.,
799   Smolenski, R.T., and Mielcarek, M. (2016). An impaired metabolism of nucleotides
800   underpins a novel mechanism of cardiac remodeling leading to Huntington's disease
801   related cardiomyopathy. *Biochim Biophys Acta* 1862**,** 2147-2157.

802   Van Eyk, C.L., O'keefe, L.V., Lawlor, K.T., Samaraweera, S.E., Mcleod, C.J., Price,
803   G.R., Venter, D.J., and Richards, R.I. (2011). Perturbation of the Akt/Gsk3-beta
804   signalling pathway is common to Drosophila expressing expanded untranslated CAG,
805   CUG and AUUCU repeat RNAs. *Hum Mol Genet* 20**,** 2783-2794.

806   Warrick, J.M., Chan, H.Y., Gray-Board, G.L., Chai, Y., Paulson, H.L., and Bonini, N.M.
807   (1999). Suppression of polyglutamine-mediated neurodegeneration in Drosophila by the
808   molecular chaperone HSP70. *Nat Genet* 23**,** 425-428.

809   Wu, M.N., Ho, K., Crocker, A., Yue, Z., Koh, K., and Sehgal, A. (2009). The effects of
810   caffeine on sleep in Drosophila require PKA activity, but not the adenosine receptor. *J*
811   *Neurosci* 29**,** 11029-11037.

812   Xiao, C., Liu, N., Jacobson, K.A., Gavrilova, O., and Reitman, M.L. (2019). Physiology
813   and effects of nucleosides in mice lacking all four adenosine receptors. *PLoS Biol* 17**,**
814   e3000161.

815   Xu, C., Franklin, B., Tang, H.W., Regimbald-Dumas, Y., Hu, Y., Ramos, J., Bosch, J.A.,
816   Villalta, C., He, X., and Perrimon, N. (2020). An in vivo RNAi screen uncovers the role
817   of AdoR signaling and adenosine deaminase in controlling intestinal stem cell activity.
818   *Proc Natl Acad Sci U S A* 117**,** 464-471.

819   Zurovec, M., Dolezal, T., Gazi, M., Pavlova, E., and Bryant, P.J. (2002). Adenosine
820   deaminase-related growth factors stimulate cell proliferation in Drosophila by depleting
821   extracellular adenosine. *Proc Natl Acad Sci U S A* 99**,** 4403-4408.

822